MgcRacGAP controls the assembly of the contractile ring and the initiation of cytokinesis

Wei-meng Zhao and Guowei Fang*

Department of Biological Sciences, Stanford University, Stanford, CA 94305-5020

Edited by Raymond L. Erikson, Harvard University, Cambridge, MA, and approved August 1, 2005 (received for review May 19, 2005)

Initiation of cytokinesis requires the establishment of the cleavage plane, the assembly of the contractile ring, and the ingression of the cleavage furrow. MgcRacGAP, a GTPase-activating protein for RhoA, is required for cytokinesis, but the mechanism of its action remains unknown. We report here that MgcRacGAP is required for the assembly of anillin and myosin into the contractile ring. In addition, MgcRacGAP is required for the localized activation of myosin through the RhoA-mediated phosphorylation of the myosin regulatory light chain. Cells with MgcRacGAP RNA interference (RNAi) failed cytokinesis without any ingression of the cleavage furrow. Paradoxically, MgcRacGAP, a GTPase-activating protein, associates during cytokinesis with ECT2, a guanine nucleotide exchange factor for RhoA, and the localization of ECT2 to both the central spindle and the contractile ring depends on MgcRacGAP. Knockdown of ECT2 phenocopies that of MgcRacGAP. We conclude that MgcRacGAP controls the initiation of cytokinesis by regulating ECT2, which in turn induces the assembly of the contractile ring and triggers the ingression of the cleavage furrow.

ECT2 | MKLP1 | myosin | RhoA | cell division

Cytokinesis, the division of a cell, requires concerted action of the central spindle, the actin cytoskeleton, and motor proteins such as myosin. Initiation of cytokinesis involves the establishment of the cleavage plane, the assembly of the contractile ring, and the ingression of the cleavage furrow. In the first step of cytokinesis, the position of the cleavage furrow is specified. Subsequently, a contractile ring, consisting of anillin, actin, myosin, formin, and septin, among other proteins, is assembled in an ordered fashion at the future cleavage site (1, 2). It is still not clear what signal initiates this assembly.

Once the contractile ring is assembled, contractile force is generated by non-muscle myosin II. The activity of myosin II is regulated by the phosphorylation of its regulatory light chain (MRLC) on threonine 18 and serine 19 (3), and overexpression of nonphosphorylatable mutants of MRLC causes defects in cytokinesis (4). Under the control of RhoA-GTP, two kinases, Rho-kinase/ROCK and citron kinase, have been shown to phosphorylate MRLC and to inhibit the MRLC phosphatase, leading to the activation of myosin motor activity (5, 6). Thus, the small GTPase RhoA, which accumulates at the cleavage furrow (7), seems to be a key upstream regulator of contractility because both inactivation and constitutive activation of RhoA lead to a failure in the constriction of the cleavage furrow (8). The activity of RhoA is under the control of a guanine nucleotide exchange factor (GEF) ECT2, a proto-oncogene initially identified through its transforming activity (9, 10). Human ECT2 is localized to the central spindle, and both antibody injection and RNA interference (RNAi) experiments showed that ECT2 is required for cytokinesis (11, 12). Similarly, Pebble, the *Drosophila* ortholog of ECT2, is associated with the cleavage furrow, and mutations in or depletion of Pebble result in failed cytokinesis (13–15).

The central spindle also plays an important role in furrow ingression (16). An evolutionarily conserved complex, centralspindlin, is critical for the structure of the central spindle (17). Centralspindlin consists of the mitotic kinesin MKLP1 and the GTPase-activating protein MgcRacGAP. Centralspindlin promotes microtubule bundling *in vitro* and is required for cytokinesis *in vivo* (17). However, the exact mechanism of centralspindlin function in cytokinesis remains to be characterized. In *Drosophila*, the centralspindlin complex is reported to form a ring-like structure that abuts or overlaps the contractile ring (13). Interestingly, RacGAP50C, the *Drosophila* ortholog of MgcRacGAP, interacts with Pebble, linking the centralspindlin complex to the ECT2 pathway (18).

In an *in vitro* small-pool-expression screen, we identified MgcRacGAP as a substrate of the anaphase-promoting complex/cyclosome, a ubiquitin ligase that controls mitotic progression (data not shown). We will report the degradation of MgcRacGAP in a separate study. In this article, we set out to determine the mechanism of MgcRacGAP function during cytokinesis and report here that MgcRacGAP is required for the assembly of the contractile ring and for the initiation of cytokinesis. We also found that centralspindlin complex specifically associates with ECT2 during anaphase and cytokinesis, and the localization of ECT2 is under the control of centralspindlin. Knockdown of ECT2 phenocopies that of MgcRacGAP, because both lead to the absence of a contractile ring and a lack of furrow ingression. We conclude that MgcRacGAP is a master regulator for initiation of cytokinesis that controls the assembly of the contractile ring and the ingression of the cleavage furrow.

Materials and Methods

Antibodies. His-tagged anillin aa454–724 and MgcRacGAP aa191–390 were expressed in *Escherichia coli*, purified by Ni-agarose, and used to immunize rabbits for production of antisera. Antibodies were affinity-purified with respective antigens. Anti-CHO1 antibody is a gift from Dr. R. Kuriyama. The following antibodies were from commercial sources: anti-nonmuscle myosin antibody (Biochemical Technologies, Stoughton, MA); anti-phospho-myosin light chain 2 (Ser-19) antibody (Cell Signaling Technology, Beverly, MA); and anti-ECT2, anti-MKLP1, anti-RhoA, anti-p38MAPK, and anti-Hsp70 antibodies (Santa Cruz Biotechnology). Anti-β-tubulin E7 monoclonal antibody was obtained from the Developmental Studies Hybridoma Bank, Iowa City, IA.

RNAi. For RNAi of ECT2, MgcRacGAP, and MKLP1, DNA-based pSUPER constructs (28) were transfected into HeLa cells by using Lipofectamine 2000 (Invitrogen). Two RNAi target sequences are used for each gene: ECT2, 5′-GCAGAGCCTTGTTGAACTTCT-3′ and 5′-CCTTGCACCAGAGGAGATTAA-3′; MgcRacGAP, 5′-GCTGAAGCATGCACGTAATCA-3′ and 5′-TCGAAGCTGTGTCCACTATTG-3′; and

This paper was submitted directly (Track II) to the PNAS office.

Abbreviations: DIC, differential interference contrast; MRLC, myosin regulatory light chain; p-MRLC, MRLC phosphorylated at Ser-19; RNAi, RNA interference.

*To whom correspondence should be addressed at: Department of Biological Sciences, Stanford University, 337 Campus Drive, Lokey Chemical Biology Building, Room 137, Stanford, CA 94305-5020. E-mail: gwfang@stanford.edu.

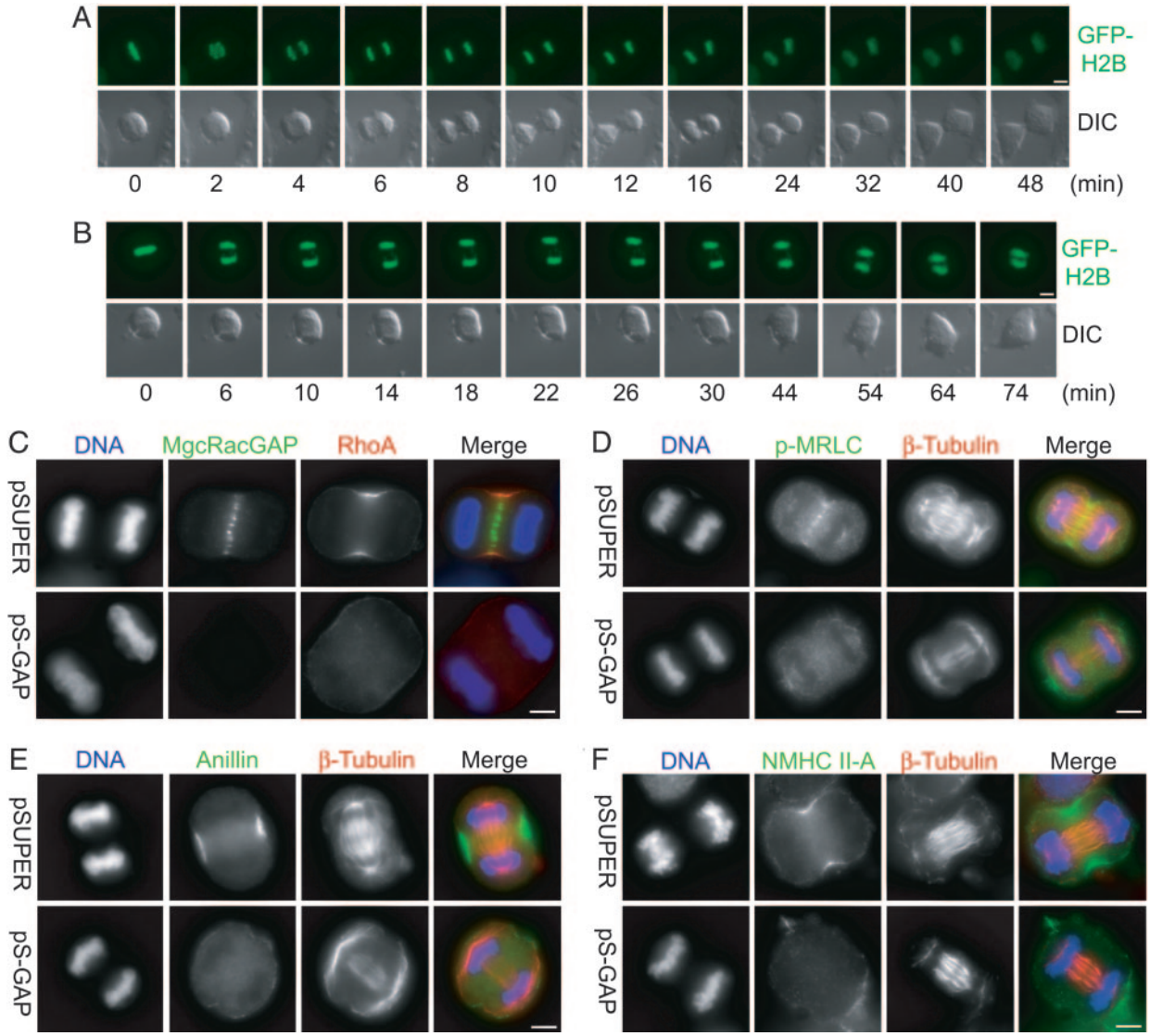

Fig. 1. MgcRacGAP is required for the initiation of cytokinesis. (*A* and *B*) Selected frames from time-lapse movies of HeLa cells stably expressing GFP-Histone H2B. Cells were transfected with either pSUPER (*A*, also see Movies 1 and 2) or pSUPER-MgcRacGAP (pS-GAP) (*B*, also see Movies 3 and 4) and imaged every minute starting from 30 h posttransfection. Both DIC and green fluorescence images were recorded and shown. (Scale bar, 10 μm.) (*C–F*) Cells were transfected with pSUPER or pS-GAP and immunostained for antigens indicated. The color of the antigen was labeled in each panel. Note that the different β-tubulin staining patterns in *D*, *E*, and *F* were due to different fixation methods used: 4% paraformaldehyde (*D* and *E*) and 4% paraformaldehyde/0.5% glutaraldehyde (*F*). (Scale bar, 5 μm.)

MKLP1, 5′-AGGTTGATGCCTTATTAGAAC-3′ and 5′-CCATAGCGTGTTCAACATTAA-3′.

Immunoprecipitation. Antibodies against ECT2 and MgcRacGAP were covalently coupled to Affi-Prep Protein A beads (Bio-Rad) at a concentration of 0.3 mg/ml. Pellets of HeLa S3 cells from various cell cycle stages were lyzed in Nonidet P-40 lysis buffer (50 mM Tris·HCl, pH 8.0/140 mM NaCl/1% Nonidet P-40/10% glycerol/0.1 mM EDTA/1 mM DTT/0.5 μM microcystin/10 μg/ml each of leupeptin, pepstatin, and chymostatin). Lysates were centrifuged and then incubated at 4°C for 1 h with Protein A beads that had been coupled with preimmune rabbit IgG. The precleared lysates were then incubated at 4°C overnight with Protein A beads that had been coupled to anti-ECT2 or MgcRacGAP antibody. Beads were recovered by centrifugation, washed five times with lysis buffer, and analyzed by immunoblotting with appropriate antibodies.

Immunofluorescence and Time-Lapse Video Microscopy. To determine localization of RhoA with the anti-RhoA antibody, cells growing on glass coverslips were fixed with ice-cold 10% trichloroacetic acid for 15 min (7). For immunofluorescence staining with myosin, cells were fixed with 4% paraformaldehyde/0.5% glutaraldehyde. For immunofluorescence staining with other antibodies, cells were fixed with 4% paraformaldehyde at room temperature for 15 min or with methanol at −20°C. After fixation, cells were permeabilized and blocked with PBS-BT (1× PBS/0.1% Triton X-100/3% BSA) at room temperature for 30 min. Coverslips were subsequently incubated in primary and secondary antibodies diluted in PBS-BT. Images were acquired with OPENLAB 4.0.2 (Improvision, Lexington, MA) under a Zeiss Axiovert 200M microscope by using ×63 or ×100 oil immersion lenses. Deconvolved images were obtained by using AUTODEBLUR 9.1 and AUTOVISUALIZER 9.1 (AutoQuant Imaging, Troy, NY). We noticed that the localization of ECT2

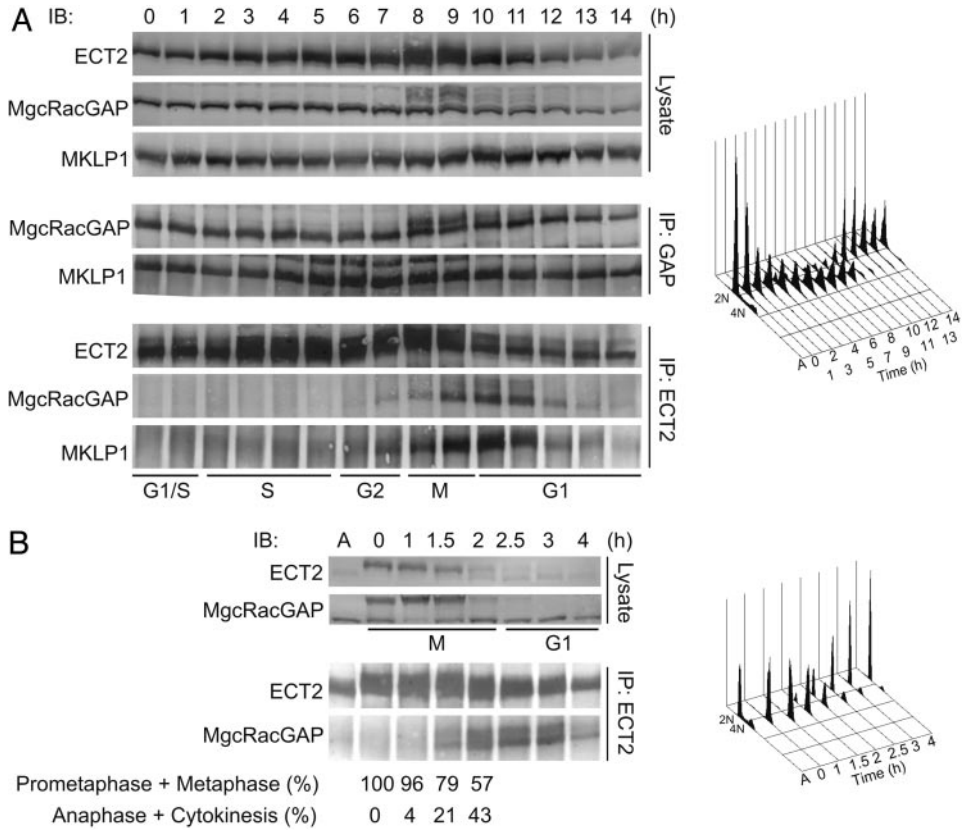

Fig. 2. Centralspindlin associates with ECT2 during cytokinesis. HeLa S3 cells were released from a double-thymidine block (*A*) or from a thymidine-nocodazole block (*B*). Lysates of synchronized HeLa S3 cells were immunoprecipitated (IP) with anti-ECT2 (*A* and *B*) or anti-MgcRacGAP (GAP) (*A*) antibodies and analyzed by immunoblotting (IB). A, asynchronous cells. Cell cycle profiles were determined by FACS analysis (*Right*). To analyze the kinetics of mitotic exit upon release from the nocodazole arrest, we divided mitotic cells into two groups: cells in prometaphase and metaphase, and cells in anaphase and cytokinesis. The number of cells in each group ($n = 200$) was counted, and the percentage of each group at different time points was listed (*B*).

depends on fixation methods used. ECT2 was only observable at the central spindle with methanol fixation, whereas ECT2 was localized both to the central spindle and to the cleavage furrow with paraformaldehyde fixation.

For time-lapse microscopy, HeLa cells stably expressing GFP-Histone H2B were cultured in Leibovitz's L-15 medium (Invitrogen) supplemented with 10% FBS (Invitrogen) and 2 mM L-glutamine (Invitrogen). Cells were placed in a 37°C heated microscope chamber and observed under differential interference contrast (DIC) and green fluorescence channel on a Zeiss Axiovert 200M microscope with a ×20 lens plus a ×1.6 Optovar. Images were acquired every minute with OPENLAB 4.0.2 software (Improvision, Lexington, MA).

Results

MgcRacGAP Is Required for the Initiation of Cytokinesis. We first determined the phase of cytokinesis in which MgcRacGAP functions. HeLa cells stably expressing GFP-Histone H2B were used in this experiment. Cells were transfected with pSUPER-MgcRacGAP, which expressed a short hairpin RNA targeting the MgcRacGAP transcript. Two different pSUPER constructs were used for each gene studied in this report to rule out potential off-target effects of RNAi. Both constructs for each gene gave the same phenotypes, and the results from only one construct were shown. At the 48th hour posttransfection, the level of MgcRacGAP was reduced by 95% (Fig. 5*A*, which is published as supporting information on the PNAS web site). The knockdown effect was quite stable and lasted up to 72 h posttransfection.

Consistent with previous reports (13, 14, 19, 20), MgcRacGAP is required for cytokinesis: at 36 h posttransfection, >40% of knockdown cells were bi-nucleated, whereas <4% cells were bi-nucleated in control transfection. To characterize the nature of the defect, transfected cells were imaged in time lapse, under both DIC and fluorescence, starting from 30 h posttransfection. Although cells transfected with pSUPER initiated and progressed through cytokinesis with normal kinetics (Fig. 1*A*; and Movies 1 and 2, which are published as supporting information on the PNAS web site), 17 out of 20 randomly recorded cells that had been transfected with pSUPER-MgcRacGAP displayed cytokinesis defects and were divided into two classes based on the degrees of furrowing. Six of 17 cells showed no or minimal (<5%) furrow ingression (Fig. 1*B*; and Movies 3 and 4, which are published as supporting information on the PNAS web site). Eleven cells displayed partial ingression (data not shown). In all cases, chromosomes separated and anaphase occurred, but cytokinesis failed, resulting in bi-nucleated cells. The different degrees of furrowing most likely reflect the variability in the depletion of MgcRacGAP. Cells that failed to initiate furrow ingression are likely to have the highest degree of MgcRacGAP knockdown. Thus, we concluded that MgcRacGAP is required for the initiation of cleavage furrow ingression.

MgcRacGAP Is Required for the Assembly of the Contractile Ring. The lack of furrow ingression in MgcRacGAP-knockdown cells could result from a lack of the contractile ring structure. Alternatively, it could result from a lack of contraction after the assembly of the contractile ring. To differentiate between these two possi-

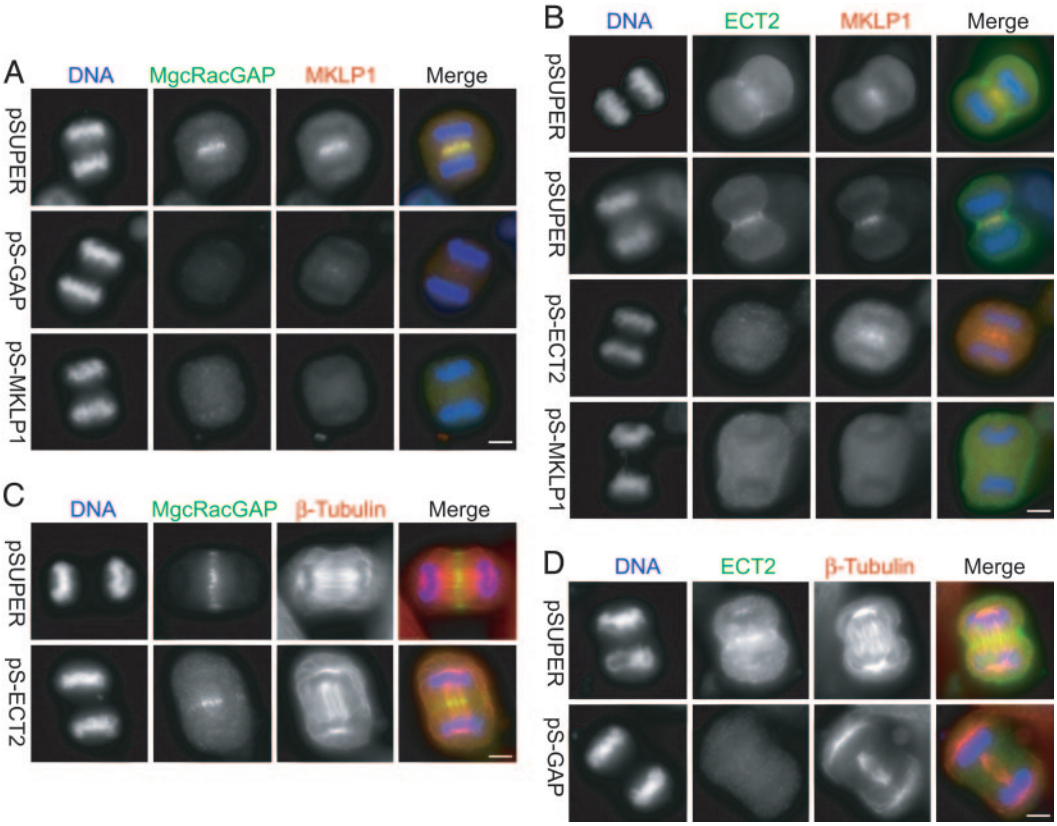

Fig. 3. Centralspindlin is required for the localization of ECT2. (*A–D*) Cells were transfected with pSUPER, pS-ECT2, pS-GAP, or pS-MKLP1 and immunostained for antigens indicated. The color of the antigen was labeled in each panel. (Scale bar, 5 μm.)

bilities, we examined in MgcRacGAP-knockdown cells the localization of contractile ring components, such as anillin, myosin, RhoA, and phosphorylated MRLC (p-MRLC, phosphorylated on Ser 19). We analyzed cells only in anaphase B and in early cytokinesis, because cells undergoing late cytokinesis were only partially depleted of MgcRacGAP.

In cells undergoing cytokinesis, MgcRacGAP was localized at the central spindle (Figs. 1*C*, and 6*A* and 7*A*, which are published as supporting information on the PNAS web site), consistent with previous reports (19, 21). In addition, we found that MgcRacGAP partially colocalized with RhoA at the contractile ring (Figs. 1*C* and 6*A*). Deconvolved images showed that MgcRacGAP existed around the cleavage furrow as punctate dots underlying the intracellular surface of the RhoA ring (Fig. 6*B*). Immunofluorescence analysis showed that, in control-transfected cells, both RhoA and p-MRLC were localized to the cleavage furrow (Fig. 1 *C* and *D*). Additionally, p-MRLC was also localized to the central spindle. Upon transfection of pSUPER-MgcRacGAP, RhoA lost its localization at the cleavage furrow in 80% of randomly selected cells ($n = 30$) undergoing anaphase B and early cytokinesis (Fig. 1*C*). In addition, 90% of randomly selected cells ($n = 20$) lost localization of p-MRLC at both the cleavage furrow and the central spindle (Fig. 1*D*). We conclude that MgcRacGAP, through targeting RhoA to the contractile ring, is required for the generation of the active contracting force at the cleavage furrow.

We next examined the localization of structural components of the contractile ring, anillin, and non-muscle myosin II-A heavy chain (NMHC II-A), both of which are targeted to the presumptive cleavage furrow at early anaphase (Fig. 1 *E* and *F*) (22–24). Surprisingly, in 90% of randomly selected anaphase and early cytokinesis cells that had been transfected with pSUPER-MgcRacGAP, neither NMHC II-A nor anillin was recruited to the presumptive cleavage furrow (Fig. 1 *E* and *F*; $n = 18$ and 16, respectively). On the other hand, knockdown of MgcRacGAP did not alter the actin staining around the cleavage furrow (data not shown). We conclude that MgcRacGAP not only is required for triggering contraction through activation of myosin phosphorylation, but more importantly is required for the assembly of the contractile ring through recruiting or maintaining anillin and myosin to the contractile ring.

MgcRacGAP Associates with ECT2 at Anaphase and During Cytokinesis. We then investigated how MgcRacGAP controls the initiation of cytokinesis, both biochemically and at the cellular level. MgcRacGAP forms a centralspindlin complex with the mitotic kinesin MKLP1 (17). We analyzed the regulation of the centralspindlin complex in the cell cycle. HeLa S3 cells were synchronized at the G_1/S boundary by a double-thymidine block, released into fresh media, and harvested every hour as described (25). The cell cycle profile of the time points was determined by FACS (Fig. 2*A*), and the time window for mitosis was identified by the presence of phosphorylated Histone H3 (data not shown). Western blot analysis indicated that the levels of MgcRacGAP and MKLP1 were constant throughout the cell cycle. We then analyzed the centralspindlin complex in the cell cycle by immunoprecipitating MgcRacGAP followed by Western blotting with an anti-MKLP1 antibody. Constant levels of MKLP1 were detected in MgcRacGAP immunoprecipitates throughout the cell cycle (Fig. 2*A*), indicating that the centralspindlin complex is constitutive in the cell cycle.

Because RacGAP50C, the *Drosophila* homolog of MgcRacGAP, interacts with Pebble both genetically as well as in a yeast two-hybrid assay (13), we tested whether centralspindlin directly

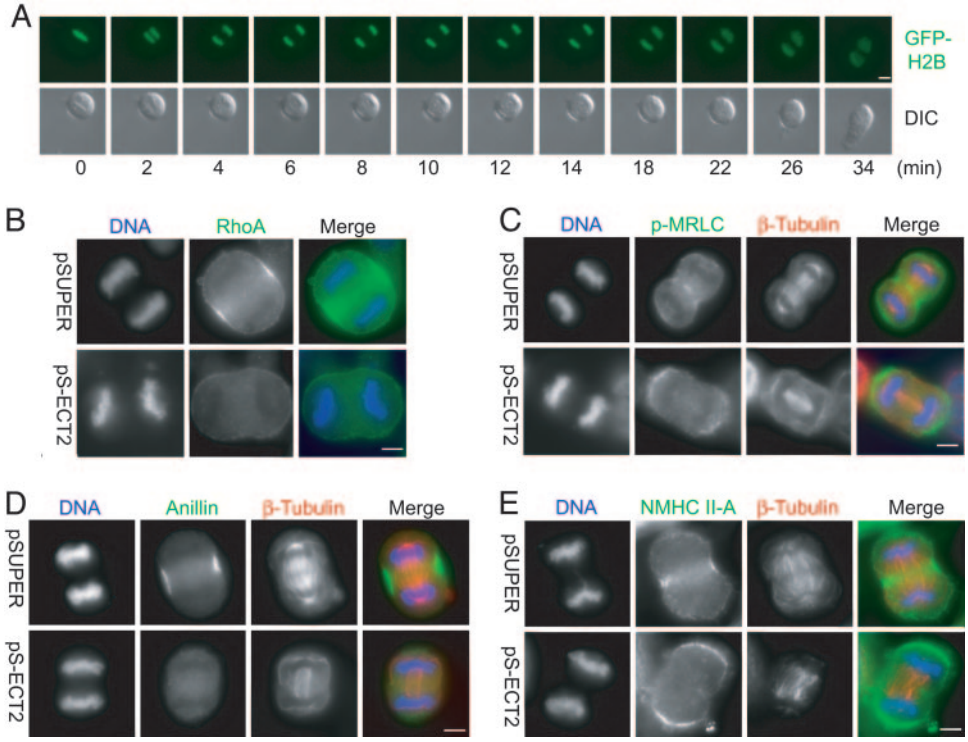

Fig. 4. ECT2 is required for the initiation of cytokinesis. (*A*) Selected frames from a time-lapse movie of HeLa/GFP-Histone H2B cells transfected with pS-ECT2 (also see Movies 5 and 6). The cell was imaged 30 h posttransfection, and both DIC and green fluorescence images are shown. (Scale bar, 10 μm.) (*B–E*) Cells were transfected with pSUPER or pS-ECT2 and immunostained for antigens indicated. The color of the antigen was labeled in each panel. (Scale bar, 5 μm.)

interacts with ECT2 during the cell cycle in mammalian cells. In HeLa S3 cells released from double-thymidine arrest, ECT2 levels fluctuate during the cell cycle, peaking in mitosis and dropping at G_1 (Fig. 2*A*). Next, ECT2 was immunoprecipitated with an anti-ECT2 antibody, and the immune-complexes were analyzed by blotting with anti-ECT2, MgcRacGAP, and MKLP1 antibodies. In S and G_2 cells, no association between centralspindlin and ECT2 was detectable (Fig. 2*A*). Interestingly, a high level of association between centralspindlin and ECT2 was observed in late mitosis, and this association disappeared 2 h after cells exited from mitosis (Fig. 2*A*). To determine the exact timing of association as well as the dissociation of centralspindlin and ECT2, we synchronized HeLa S3 cells at prometaphase by a thymidine-nocodazole block (25) and then released cells from mitosis into G_1 (Fig. 2*B*). Association between ECT2 and MgcRacGAP was not detectable in asynchronized cells and in cells at prometaphase and metaphase (cell samples collected during the first hour postrelease) (Fig. 2*B*). Strong association between MgcRacGAP and ECT2 was detected when the cells passed through anaphase and cytokinesis, and the level of the MgcRacGAP-ECT2 complex peaked when a majority of cells undergo anaphase/cytokinesis and exit into G_1 (cell samples collected 2–3 h postrelease) (Fig. 2*B*). Thus, centralspindlin associates with ECT2, and the kinetics of the initial formation of this complex coincide with the initiation of cytokinesis, suggesting that formation of this complex may control the initiation of cytokinesis.

Centralspindlin Targets ECT2 to the Central Spindle and to the Cleavage Furrow. We next investigated the functional importance of the centralspindlin–ECT2 interaction. At the cellular level, MKLP1 colocalized with MgcRacGAP at anaphase and during cytokinesis (Figs. 3*A* and 6 *A* and *B*; data not shown), consistent with a previous report (21). ECT2 was also localized at the cleavage furrow and at the central spindle (Fig. 3 *B* and *D*). We then examined the interdependence of centralspindlin and ECT2 on their localization. We reduced the expression of ECT2, MgcRacGAP, and MKLP1 by RNAi. At the 48th hour posttransfection, the levels of ECT2 and MgcRacGAP were reduced by 95% in their respective knockdown samples, whereas the level of MKLP1 was reduced by 80% (Fig. 5 *A–C*). In ECT2-knockdown cells, both MKLP1 and MgcRacGAP remained on the central spindle (Fig. 3 *B* and *C*, $n = 24$ and 22, respectively), indicating that the localization of centralspindlin is independent of ECT2. On the other hand, in MgcRacGAP-knockdown cells, ECT2 was absent from the central spindle and from the cleavage furrow at anaphase B and in early cytokinesis (Fig. 3*D*, $n = 25$). Similarly, in MKLP1 knockdown cells, ECT2 was also absent from the central spindle and from the cleavage furrow (Fig. 3*B*, $n = 20$). Thus, centralspindlin controls the localization of ECT2 to the central spindle and to the cleavage furrow.

Interestingly, in MKLP1-knockdown cells ($n = 23$), MgcRacGAP is also absent from the central spindle (Fig. 3*A*), consistent with a previous report on RacGAP50C in *Drosophila* (13). On the other hand, in MgcRacGAP-knockdown cells ($n = 18$), a weak signal of MKLP1 (≈20% intensity of that found in control transfected cells) remained at the central spindle (Fig. 3*A*). This observation suggested the existence of a MgcRacGAP-independent mechanism for localization of MKLP1 to the central spindle, although we cannot exclude the possibility that residual MgcRacGAP, beyond our detection limit by immunofluorescence staining, persists and is sufficient for MKLP1 localization in MgcRacGAP-knockdown cells. We conclude that the central spindle localization of MgcRacGAP depends on MKLP1, but the localization of MKLP1 may only partially depend on MgcRacGAP.

ECT2 Controls the Assembly of the Contractile Ring and the Initiation of Cytokinesis. To analyze the function of ECT2 during cytokinesis, we imaged ECT2-knockdown cells by time-lapse micros-

copy. In 40% of ECT2-knockdown cells recorded undergoing anaphase and early cytokinesis ($n = 30$), the cell division failed without any ingression of the cleavage furrow (Fig. 4*A*; and Movies 5 and 6, which are published as supporting information on the PNAS web site), similar to the phenotype of MgcRacGAP-deficient cells. In the remaining 60% of knockdown cells, the cleavage furrow partially ingressed, but then regressed (data not shown). This variability in furrow ingression most likely reflects the different degree of knockdown.

We then analyzed the cleavage furrow structure in fixed cells. In ECT2 knockdown cells, all contractile ring components examined [RhoA, p-MRLC, anillin, and non-muscle myosin II-A heavy chain (NMHC II-A)] were absent from the presumptive cleavage furrow (Fig. 4 *B–E*), indicating a lack of the contractile ring structure. In addition, the central spindle structure was much narrower in ECT2-knockdown cells than in control cells (Fig. 4 *C–E*). This observation was better demonstrated with deconvolved images (Fig. 7 *A* and *B*). We conclude that, like MgcRacGAP, ECT2 is required for the assembly of the contractile ring and the initiation of cytokinesis.

Discussion

Although previous studies (17, 19) suggest a requirement of MgcRacGAP in cytokinesis, we report here that MgcRacGAP specifically controls the initiation of cytokinesis in mammalian cells. Time-lapse analysis revealed no furrow ingression in human cells with knockdown of MgcRacGAP, even though chromosomes separated and anaphase occurred normally (Fig. 1). At the cellular level, MgcRacGAP is required for the activation of the myosin motor and for the initiation of furrow ingression. In the absence of MgcRacGAP, RhoA and p-MRLC (two activators of the myosin motor) are not concentrated at the presumptive furrow in anaphase B and during early cytokinesis. More importantly, MgcRacGAP is required for the assembly of the contractile ring structure. In the absence of MgcRacGAP, two components of the contractile ring (anillin and non-muscle myosin II heavy chain) fail to assemble into the presumptive cleavage furrow at anaphase, indicating a lack of the contractile ring structure (Fig. 1).

The following evidence indicates that MgcRacGAP controls the initiation of cytokinesis through ECT2. First, MgcRacGAP associates with ECT2, but only during mitotic exit and cytokinesis (Fig. 2). Second, the localization of ECT2 to the central spindle and to the cleavage furrow depends on MgcRacGAP, whereas the localization of MgcRacGAP is independent of ECT2 (Fig. 3). Third, knockdown of ECT2 generates an identical phenotype as knockdown of MgcRacGAP: the contractile ring fails to assemble and cytokinesis fails without any furrow ingression (Fig. 4).

We conclude that, during cytokinesis, MgcRacGAP controls ECT2, which, in turn, induces the assembly of the contractile ring and triggers the ingression of the cleavage furrow. It is surprising to discover that the guanine nucleotide exchange factor ECT2, a positive regulator of RhoA, is under the direct control of the GTPase-activating protein MgcRacGAP, a negative regulator of RhoA. This apparent paradox can be reconciled by the fact that MgcRacGAP has a GAP activity toward Cdc42 (26), but not toward RhoA during early cytokinesis. Activation of its GAP activity for RhoA requires phosphorylation of MgcRacGAP by the aurora B kinase (27), which occurs only when the ingression of the cleavage furrow approaches to completion. We speculate that the centralspindlin complex mainly functions as a targeting factor at anaphase B to recruit, and also possibly to activate, ECT2 at the central spindle and at the contractile ring, leading to the activation of RhoA and the initiation of cytokinesis.

We thank Dr. Ryoko Kuriyama (University of Minnesota, Minneapolis) for the anti-CHO1 antibody, Akiko Seki for purifying the anti-MgcRacGAP antibody, and members of the G.F. laboratory for discussions. W.-m.Z. was supported by a postdoctoral fellowship from the American Heart Association. This work was supported by a Burroughs-Wellcome Career Award in Biomedical Sciences and by National Institutes of Health Grant GM062852 (to G.F.).

1. Glotzer, M. (2004) *J. Cell Biol*. **164,** 347–351.
2. Wu, J. Q., Kuhn, J. R., Kovar, D. R. & Pollard, T. D. (2003) *Dev. Cell* **5,** 723–734.
3. Yamakita, Y., Yamashiro, S. & Matsumura, F. (1994) *J. Cell Biol*. **124,** 129–137.
4. Komatsu, S., Yano, T., Shibata, M., Tuft, R. A. & Ikebe, M. (2000) *J. Biol. Chem*. **275,** 34512–34520.
5. Yamashiro, S., Totsukawa, G., Yamakita, Y., Sasaki, Y., Madaule, P., Ishizaki, T., Narumiya, S. & Matsumura, F. (2003) *Mol. Biol. Cell* **14,** 1745–1756.
6. Kosako, H., Yoshida, T., Matsumura, F., Ishizaki, T., Narumiya, S. & Inagaki, M. (2000) *Oncogene* **19,** 6059–6064.
7. Hayashi, K., Yonemura, S., Matsui, T. & Tsukita, S. (1999) *J. Cell Sci*. **112,** 1149–1158.
8. Drechsel, D. N., Hyman, A. A., Hall, A. & Glotzer, M. (1997) *Curr. Biol*. **7,** 12–23.
9. Kimura, K., Tsuji, T., Takada, Y., Miki, T. & Narumiya, S. (2000) *J. Biol. Chem*. **275,** 17233–17236.
10. Miki, T., Smith, C. L., Long, J. E., Eva, A. & Fleming, T. P. (1993) *Nature* **362,** 462–465.
11. Tatsumoto, T., Xie, X., Blumenthal, R., Okamoto, I. & Miki, T. (1999) *J. Cell Biol*. **147,** 921–928.
12. Kim, J. E., Billadeau, D. D. & Chen, J. (2004) *J. Biol. Chem*. **280,** 5733–5739.
13. Somers, W. G. & Saint, R. (2003) *Dev. Cell* **4,** 29–39.
14. Somma, M. P., Fasulo, B., Cenci, G., Cundari, E. & Gatti, M. (2002) *Mol. Biol. Cell* **13,** 2448–2460.
15. Prokopenko, S. N., Brumby, A., O'Keefe, L., Prior, L., He, Y., Saint, R. & Bellen, H. J. (1999) *Genes Dev*. **13,** 2301–2314.
16. Inoue, Y. H., Savoian, M. S., Suzuki, T., Mathe, E., Yamamoto, M. T. & Glover, D. M. (2004) *J. Cell Biol*. **166,** 49–60.
17. Mishima, M., Kaitna, S. & Glotzer, M. (2002) *Dev. Cell* **2,** 41–54.
18. Saint, R. & Somers, W. G. (2003) *J. Cell Sci*. **116,** 4277–4281.
19. Hirose, K., Kawashima, T., Iwamoto, I., Nosaka, T. & Kitamura, T. (2001) *J. Biol. Chem*. **276,** 5821–5828.
20. Jantsch-Plunger, V., Gonczy, P., Romano, A., Schnabel, H., Hamill, D., Schnabel, R., Hyman, A. A. & Glotzer, M. (2000) *J. Cell Biol*. **149,** 1391–1404.
21. Mishima, M., Pavicic, V., Gruneberg, U., Nigg, E. A. & Glotzer, M. (2004) *Nature* **430,** 908–913.
22. De Lozanne, A. & Spudich, J. A. (1987) *Science* **236,** 1086–1091.
23. Oegema, K., Savoian, M. S., Mitchison, T. J. & Field, C. M. (2000) *J. Cell Biol*. **150,** 539–552.
24. Straight, A. F., Cheung, A., Limouze, J., Chen, I., Westwood, N. J., Sellers, J. R. & Mitchison, T. J. (2003) *Science* **299,** 1743–1747.
25. Fang, G., Yu, H. & Kirschner, M. W. (1998) *Mol. Cell* **2,** 163–171.
26. Oceguera-Yanez, F., Kimura, K., Yasuda, S., Higashida, C., Kitamura, T., Hiraoka, Y., Haraguchi, T. & Narumiya, S. (2005) *J. Cell Biol*. **168,** 221–232.
27. Minoshima, Y., Kawashima, T., Hirose, K., Tonozuka, Y., Kawajiri, A., Bao, Y. C., Deng, X., Tatsuka, M., Narumiya, S., May, W. S., Jr., *et al*. (2003) *Dev. Cell* **4,** 549–560.
28. Brummelkamp, T. R., Bernards, R. & Agami, R. (2002) *Science* **296,** 550–553.